Identification of flow structures by Lagrangian trajectory methods

Tomas Torsvik

Wave Engineering Laboratory
Institute of Cybernetics at Tallinn University of Technology

Non-homogeneous fluids and flows
August 27–31, Prague

Surface water transport

Examples of sea surface transport influenced by turbulent flow.

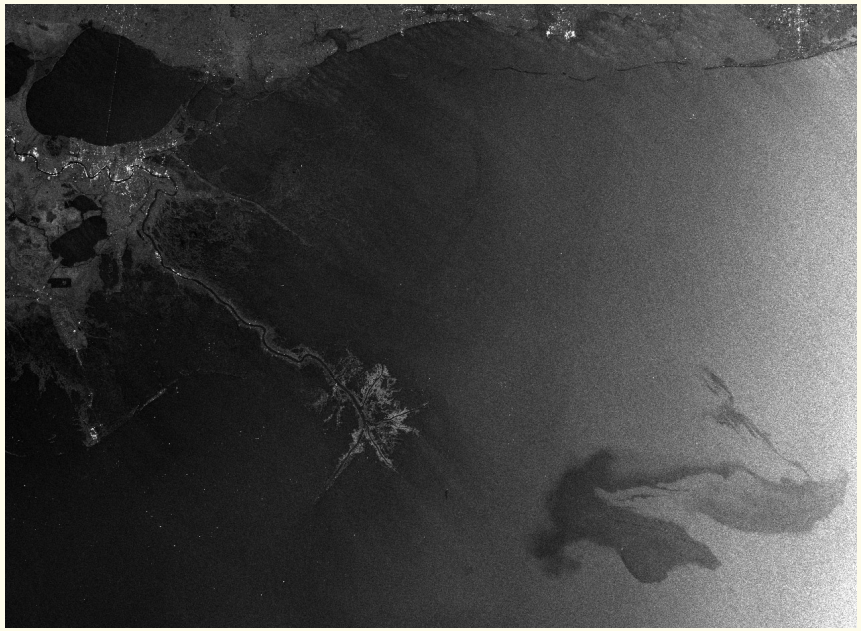

Oil spill in the Gulf of Mexico. ASAR image, 25 April 2010. Source: ESA

Blue-green algae bloom in the Baltic Sea. MERIS image, 11 July 2010.

Source: ESA

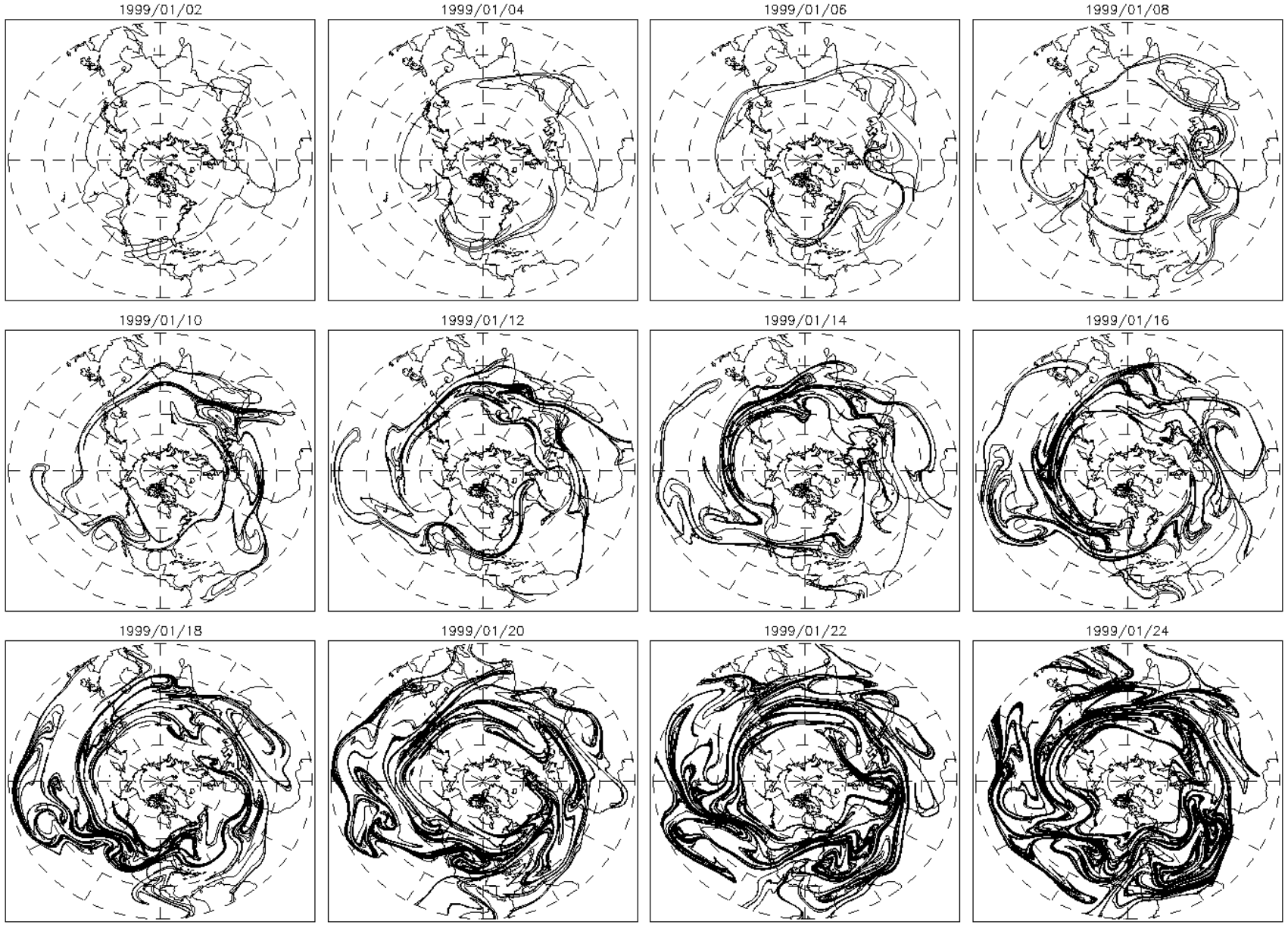

Water vapour contour, 2.4e-2 mmr, advected on a 400 K isentropic surface. Simulation in Interactive Data Language with UK Met Office (UKMO) wind fields.

The Lagrangian point of view

Eulerian point of view

velocity: $\vec{u}(\vec{x}, t)$
tracer concentration: $c(\vec{x}, t)$

The Lagrangian point of view

Eulerian point of view

velocity: $\vec{u}(\vec{x}, t)$
tracer concentration: $c(\vec{x}, t)$

Lagrangian point of view

For parcel with initial position

$$\vec{a} = \vec{x}(\vec{a}, 0)$$

position: $\vec{x}(\vec{a}, t)$
velocity: $\vec{u}(\vec{x}(\vec{a}, t), t)$
tracer concentration: $c(\vec{x}(\vec{a}, t), t)$

Experiments: Surface drifters

Drifter experiments in Gulf of Finland.

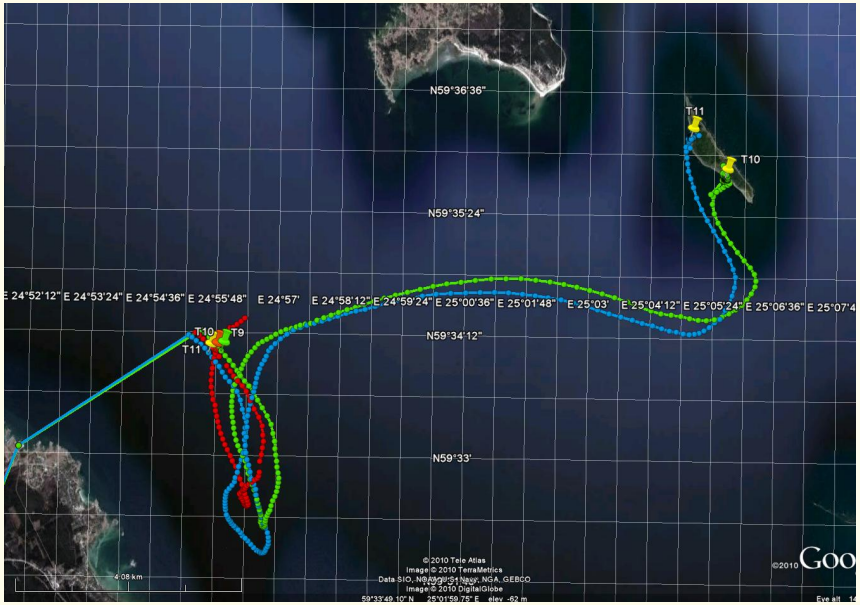

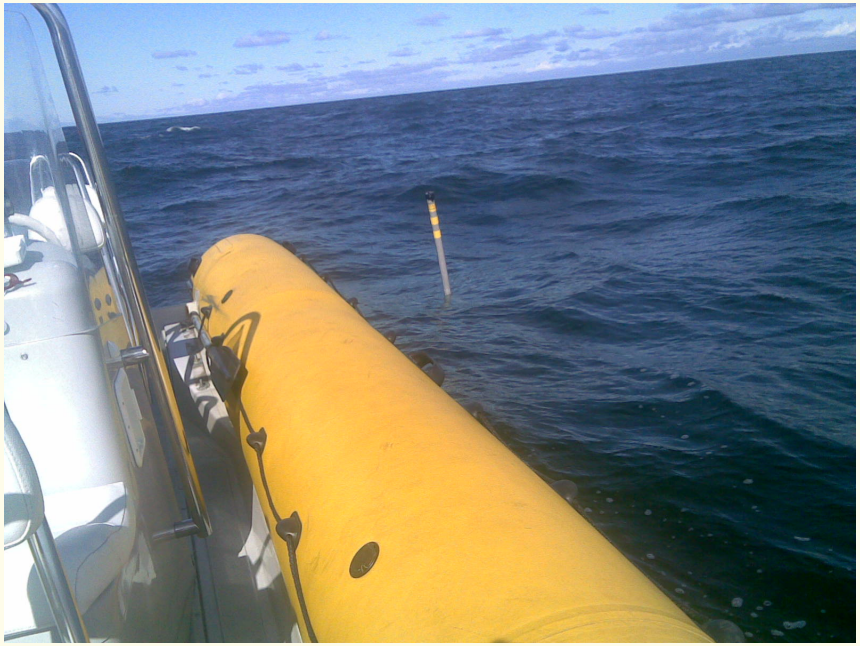

Problem: Few trajectories, high cost.

Lagrangian dispersion

Lagrangian analysis is usually based on fluid volumes, or patches, which are large compared to molecular diffusion length scale. Patch transport is diffusive if patch sizes exceed the size of the most energetic eddies.

- Small patch size compared to the eddy scale: There is little growth in the mean patch size, except for what is caused by shear within the eddy.
- Similar patch and eddy size: The patch is drawn into filaments or streaks by the eddy.
- Large patch size compared to the eddy scale: Eddies cause mixing within the patch and slowly extend the patch boundaries.

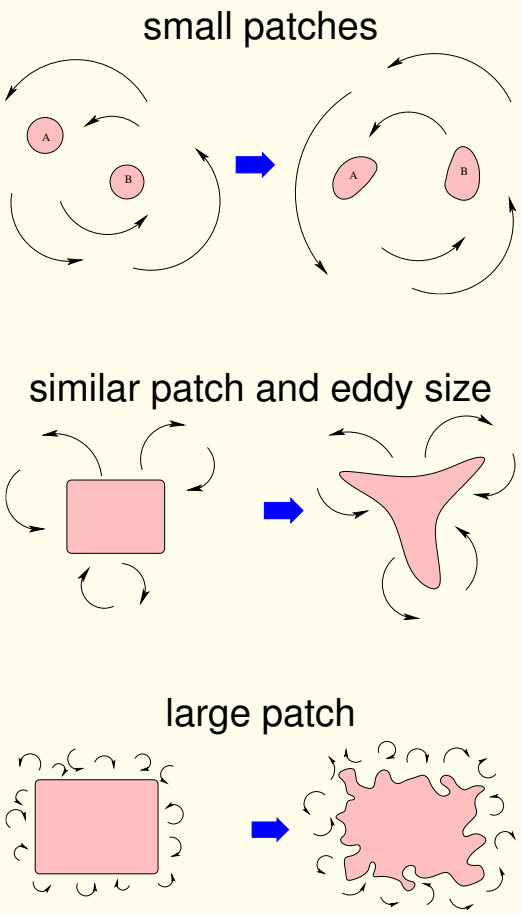

Autocorrelation and integral scales

Given a cloud of particles released at time $t = 0$, and that the location of a single particle relative to its release point is $X(t) = \int_0^t u(\tau)d\tau$. The relative spreading of particles depend on how long their motions remain similar.

A measure of the time scale over which the particle motion remains similar is provided by the *velocity autocorrelation function* $R(\tau)$, given by the mean of the product of the speeds u for a single particle, measured at two times separated by a time interval τ, normalized by the standard deviation σ_u of the particle speed

$$R(\tau) = \langle u(t)u(t+\tau)\rangle/\sigma_u^2 \equiv \left\{ \lim_{T\to\infty} \left[\frac{1}{T} \int_0^T u(t)u(t+\tau)dt \right] \right\} / \sigma_u^2$$

where

$$\sigma_u^2 = \lim_{T\to\infty} \left[\frac{1}{T} \int_0^T u^2(t)dt \right]$$

Autocorrelation and integral scales

The *Lagrangian integral time scale*

$$T_L = \int_0^\infty R(\tau) d\tau$$

measure for particle speed autocorrelation

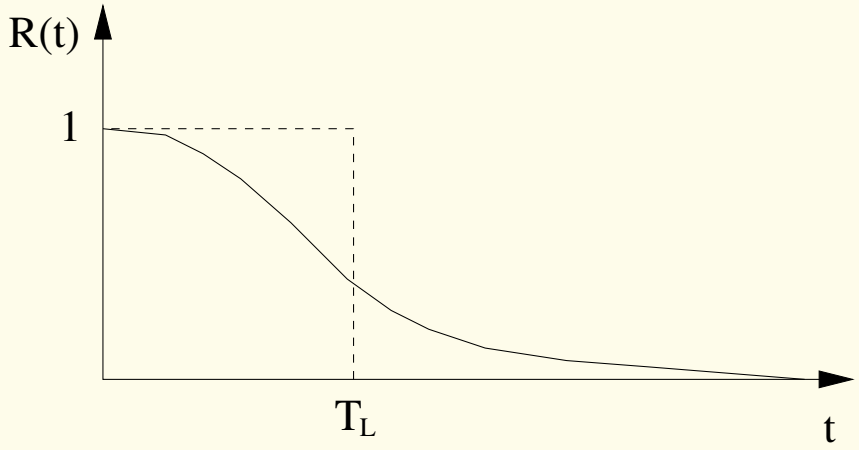

- *Lagrangian integral length scale:* $L_L = \sigma_u T_L$

In practice R is calculated from averages over many particle trajectories, often assuming spatial and temporal homogeneity of the turbulent velocity field.

- In homogeneous turbulent flow, the rate of change in variance of particle positions $\langle x^2 \rangle$ for an ensamble of particles is related to R by

$$\frac{d}{dt}\langle x^2 \rangle = 2\sigma_u^2 \int_0^t R(\tau) d\tau$$

- 'Eddy dispersion coefficient': $K_H = \frac{1}{2}(d/dt)[\langle x^2 \rangle]$

Autocorrelation and integral scales

Assume an ensamble of particles are released from a fixed location at $t = 0$.

- For $t \ll T$: The velocity autocorrelation function $R(\tau) \approx 1$

$$\frac{d}{dt}\langle x^2 \rangle \approx 2\sigma_u^2 t \quad \text{hence} \quad \langle x^2 \rangle \approx \sigma_u^2 t^2$$

  The eddy dispersion coefficient $K_H \approx \sigma_u^2 t$ increase linearly with time for $t \ll T_L$.

- At large times $t \gg T_L$:

$$\frac{d}{dt}\langle x^2 \rangle \approx 2\sigma_u^2 T_L \quad \text{hence} \quad \langle x^2 \rangle \approx 2\sigma_u^2 T_L t$$

  The eddy dispersion coefficient $K_H \approx \sigma_u^2 T_L$ is constant. In terms of the Lagrangian integral length scale the coefficient becomes

$$K_{H\infty} \approx \sigma_u L_L$$

The time T_L provides information about how long it takes to attain a constant rate of dispersion.

Model equations for Lagrangian transport

Based on theory for stochastic processes:

- C. Gardiner: “Stochastic Methods”, Springer 2010

Lagrangian Stochastic models have been used for atmospheric boundary layers since the 1970s. Increasingly used in ocean modeling for transport problems and flow characterization.

Lagrangian Stochastic models in ocean sciences:

- Dimou and Adams: “A random-walk, particle tracking model for well-mixed estuaries and coastal waters”, Estuarine Coastal and Shelf Science, 37(1):99–110, JUL 1993.
- Blumberg, Dunning, Li, Heimbuch, and Geyer: “Use of a particle tracking model for predicting entrainment at power plants on the hudson river”, Estuaries, 27(3):515–526, JUN 2004.

Model equations: Basic assumptions

- Particle trajectories can be modeled by Lagrangian Stochastic equations. The stochastic component is required to account for particle dispersion due to unresolved processes.
- The stochastic element of the motion can be described as a continuous-time, continuous state-space Markov process with continuous sample paths, in which case the evolution of the probability density function for the particle cloud is determined by the *Fokker-Planck* equation.
- The stochastic element of the motion for long term evolution of a large number of particles can be described by the Wiener process.
- Particles are assumed to behave as passive tracers, i.e. point objects at equilibrium with its surrounding water mass.

The Langevin equation

- Assume a particle is determined located at the position

$$\vec{X}(t) = (X_1, X_2, X_3) \quad \text{at time } t$$

- The drift of the particle with time is described by the Langevin equation, which has the general form

$$\frac{d\vec{X}}{dt} = A(\vec{X}, t) + B(\vec{X}, t)\xi(t)$$

$A(\vec{X}, t)$ - deterministic forces acting on the particle
$B(\vec{X}, t)$ - random forces acting on the particle
$\xi(t)$ - vector composed of random numbers

- The fundamental diffusion process is called the *Wiener process*, where the random numbers are selected from a distribution with zero mean and variance proportional to dt.
- The discrete form of the equation is

$$\Delta\vec{X}_{n+1} = \vec{X}_{n+1} - \vec{X}_n = A(\vec{X}_n, t_n)\Delta t + B(\vec{X}_n, t_n)\sqrt{\Delta t}\gamma_n$$

where γ_n is a vector of independent random numbers with zero mean and unit variance.

The Fokker-Planck equation

If we define

$$f = f(\vec{X}, t|\vec{X}_0, t_0)$$

as the conditional probability density function for the positions $\vec{X}(t)$ for particles with initial positions $\vec{X}_0$ at time t_0, the *Fokker-Planck equation*

$$\frac{\partial f}{\partial t} + \frac{\partial}{\partial \vec{X}}(Af) = \nabla^2 \left(\frac{1}{2} BB^T f \right) ,$$

determines the evolution of f in the limit as the number of particles becomes very large and the time step used to solve the transport equation becomes very small.

How do we determine A and B?

Natural choice for ocean models: make the Lagrangian trajectory model equivalent to the transport model for a passive tracer.

GCM: Tracer concentration

The transport equation for a conservative tracer C is given by the (Eulerian) advection-diffusion equation

$$\frac{\partial C}{\partial t} + \frac{\partial CU}{\partial x} + \frac{\partial CV}{\partial y} + \frac{\partial CW}{\partial z} =$$
$$\frac{\partial}{\partial x}\left(A_H \frac{\partial C}{\partial x}\right) + \frac{\partial}{\partial y}\left(A_H \frac{\partial C}{\partial y}\right) + \frac{\partial}{\partial z}\left(K_H \frac{\partial C}{\partial z}\right) ,$$

where U, V, W are velocity components, and A_H, K_H are horizontal and vertical eddy diffusivity coefficients.

Expanding the tracer transport equation by the terms

$$\frac{\partial}{\partial x}\left(C\frac{\partial A_H}{\partial x}\right)+\frac{\partial}{\partial y}\left(C\frac{\partial A_H}{\partial y}\right)+\frac{\partial}{\partial z}\left(C\frac{\partial K_H}{\partial z}\right)$$

results in a transport equation which is equivalent to the Fokker-Planck equation

$$\begin{aligned}&\frac{\partial C}{\partial t}+\frac{\partial}{\partial x}\left\{\left[U+\frac{\partial A_H}{\partial x}\right]C\right\}\\&+\frac{\partial}{\partial y}\left\{\left[V+\frac{\partial A_H}{\partial y}\right]C\right\}+\frac{\partial}{\partial z}\left\{\left[W+\frac{\partial K_H}{\partial z}\right]C\right\}\\&=\frac{\partial^2}{\partial x^2}\left(A_H C\right)+\frac{\partial^2}{\partial y^2}\left(A_H C\right)+\frac{\partial^2}{\partial z^2}\left(K_H C\right).\end{aligned}$$

The particle tracking model is consistent with the tracer transport equation if we choose

$$A \equiv \begin{bmatrix} U + \frac{\partial A_H}{\partial x} \\ V + \frac{\partial A_H}{\partial y} \\ W + \frac{\partial K_H}{\partial z} \end{bmatrix} \quad \text{and} \quad \frac{1}{2} BB^T \equiv \begin{pmatrix} A_H & 0 & 0 \\ 0 & A_H & 0 \\ 0 & 0 & K_H \end{pmatrix}$$

On component form the Lagrangian stochastic model equation corresponding to an advection-diffusion process becomes

$$\Delta X = \left(U + \frac{\partial A_H}{\partial x} \right) \Delta t + \sqrt{2 A_H \Delta t} \gamma(t)$$

$$\Delta Y = \left(V + \frac{\partial A_H}{\partial y} \right) \Delta t + \sqrt{2 A_H \Delta t} \gamma(t)$$

$$\Delta Z = \left(W + \frac{\partial K_H}{\partial z} \right) \Delta t + \sqrt{2 K_H \Delta t} \gamma(t)$$

- Transport of active and passive tracers may be calculated directly in the GCM by advection-diffusion equations.
- Transport of passive, neutrally buoyant particles is consistent with tracer transport if the Fokker-Planck equation is equivalent to the advection-diffusion equation.

Why simulate particle tracks instead of tracer concentrations?

1. Sources are more naturally represented in a particle tracking model, where new particles can easily be introduced at different times, whereas it can be difficult to resolve a point source with a concentration model.
2. A particle tracking model can provide information about the behavior or fate of individual agents, such as behavior of fish larvae under changing conditions, or settling of different size of particles.
3. Particle tracking models are also a more natural choice when we are interested in integrated properties, such as residence time, rather than the concentration distribution itself.

GCM and particle tracking

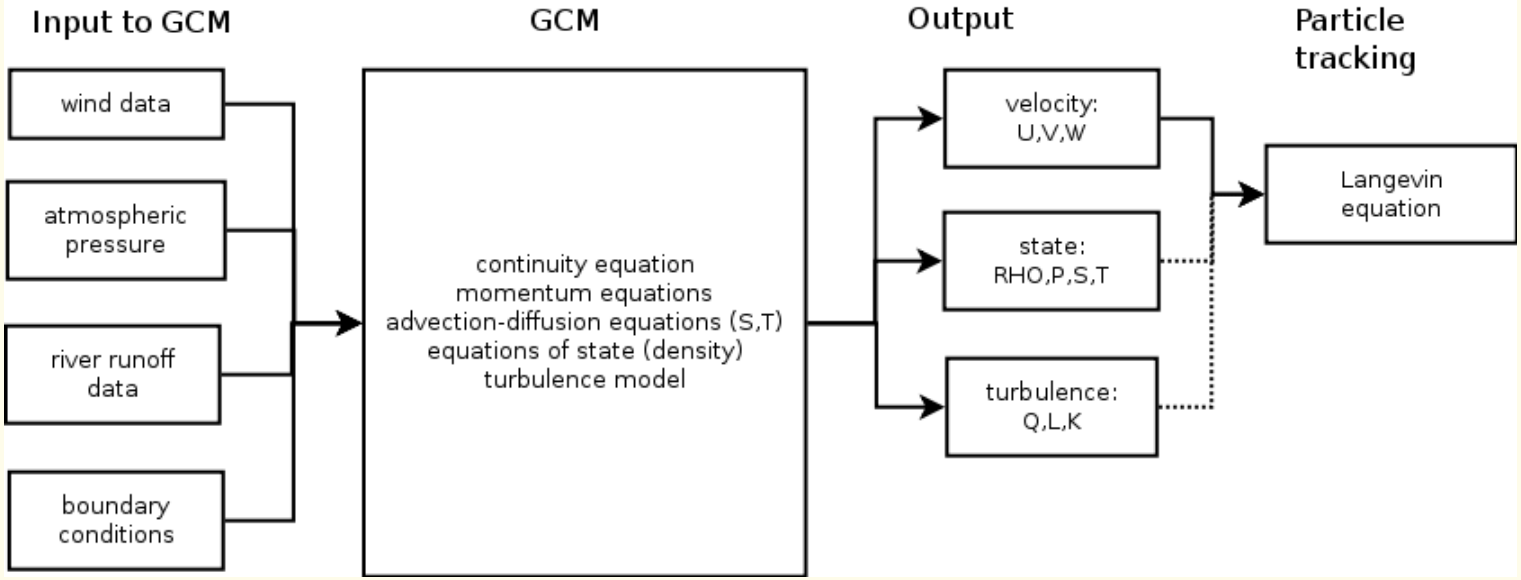

- GCM: Eulerian (field) description of flow, driven by pressure gradients.
- Particle tracking: Lagrangian (point) description of flow, driven by velocity vectors.

Example: Random particle dispersion

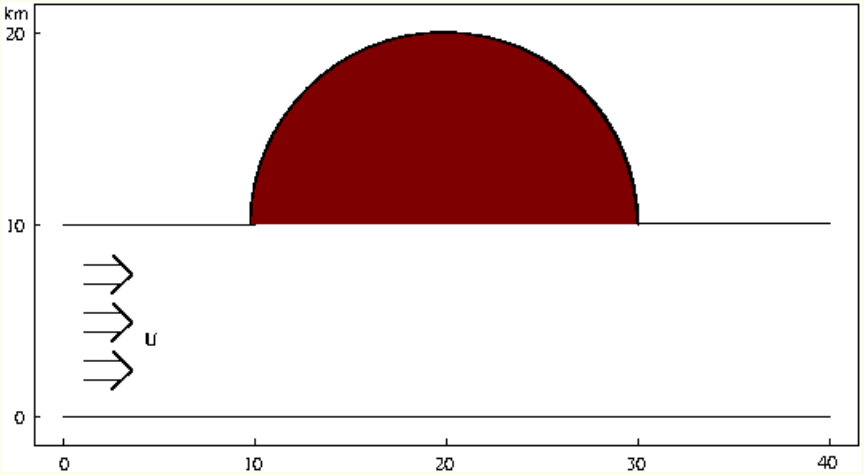

- Simulation without random dispersion: Trajectories follow streamlines and a large number of particles remain trapped near channel walls.
- Simulation with random dispersion: Boundary layer with wall-bound particles is gradually diluted.

Particle residence time within bay area:

non-dispersive simulation

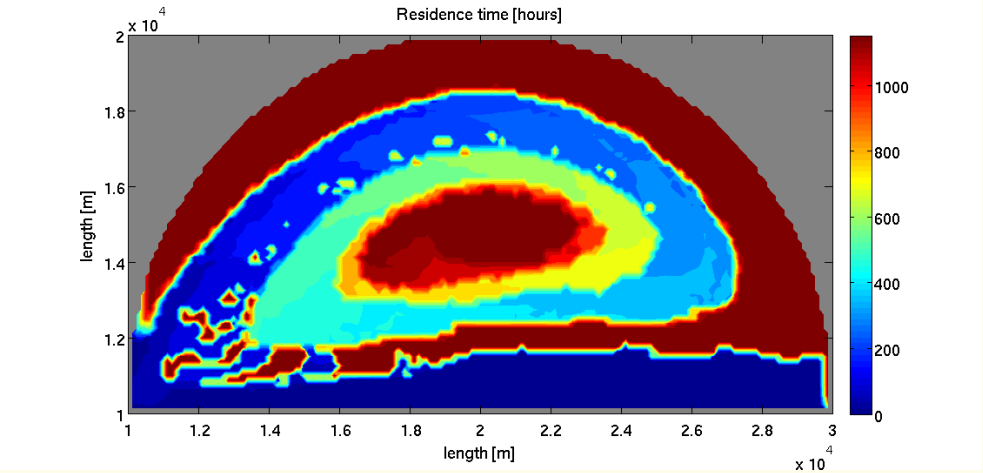

dispersive simulation

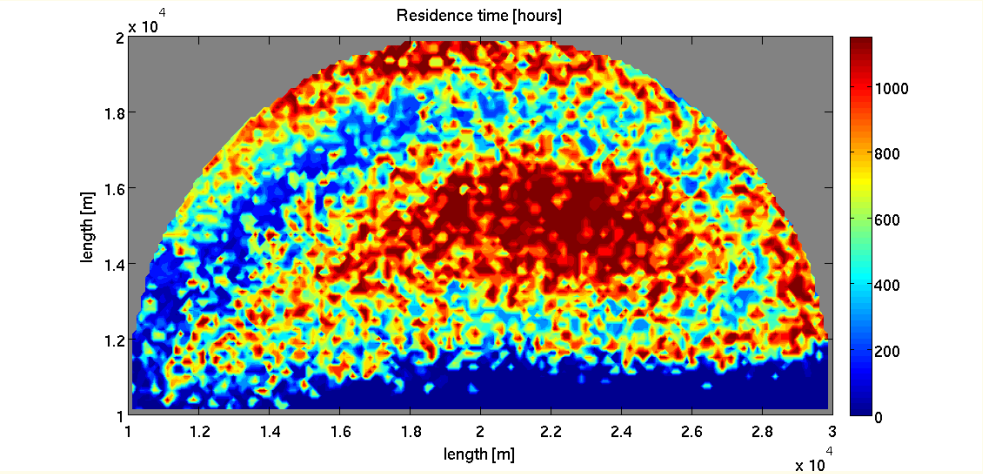

Example: Residence time

Residence time of particles in western part of Baltic Sea. Colors indicate age of particles from 1 to 20 days.

K. Doos, A. Engqvist: *Estuarine, Coastal and Shelf Science* 74 (2007)

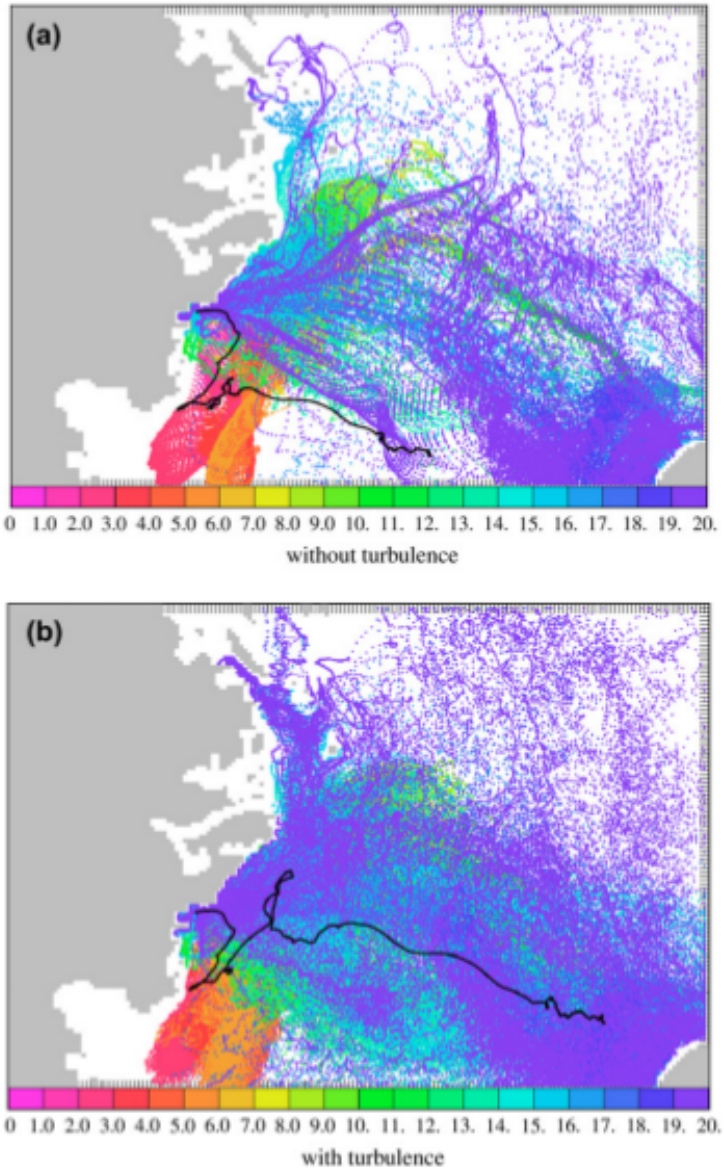

Fig. 4. 1823 Lagrangian trajectories released from the discharge regions the 15th

Example: Oil spill modeling

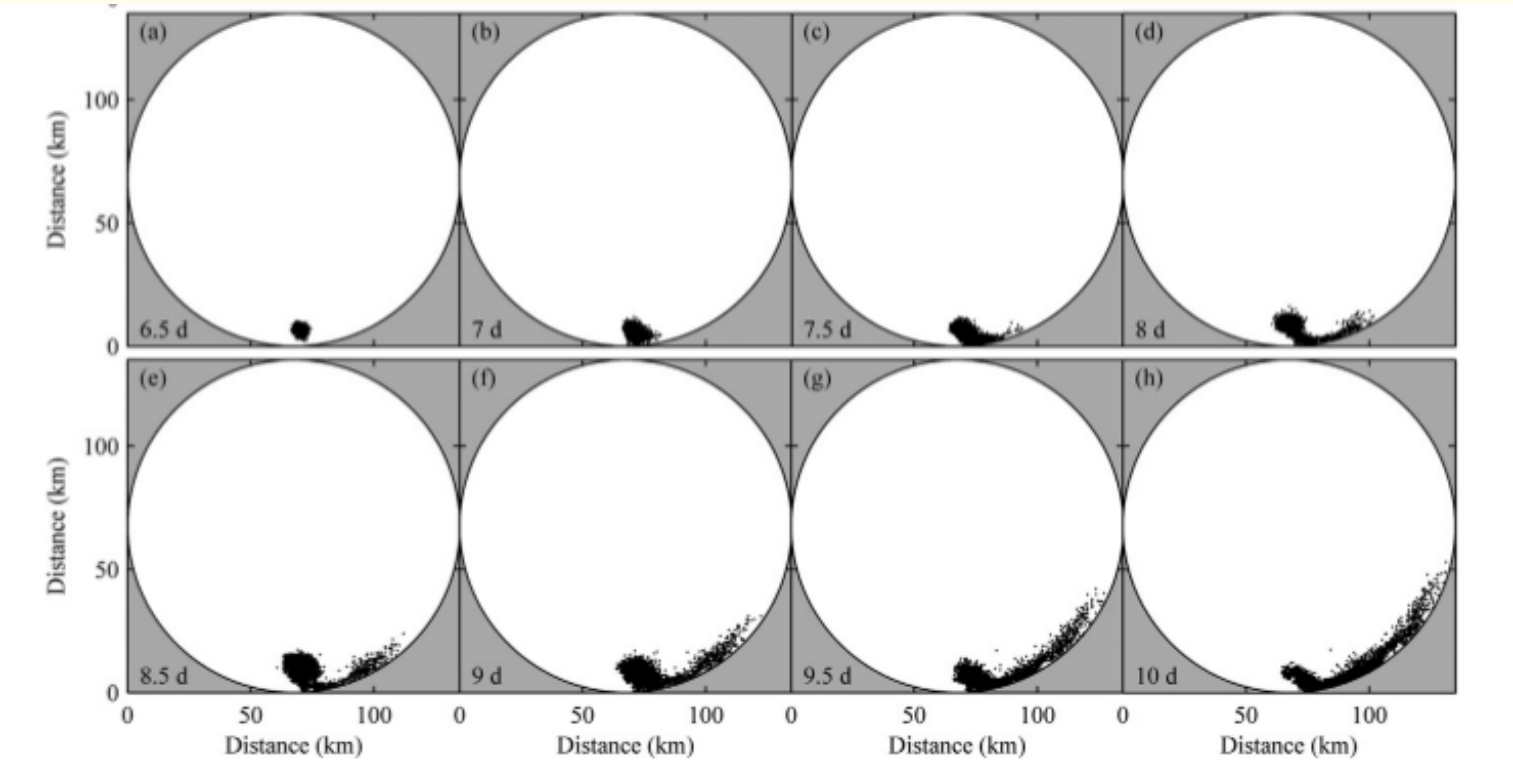

Fig. 12. Snapshots of surface oil trajectory under the flow fields supplied by flow module and ROMS using uniform Cartesian grid every 12 h after the oil spill. (1)–(8) represent the simulated trajectories under flow module; (a)–(h) represent the simulated trajectories under ROMS with Cartesian grid.

Wang, Shen *Ocean Modelling* 35 (2010) 332–344

A Lagrangian particle model can be combined with a oil spill model to simulate the evolution of an oil spill. The oil spill model accounts for effects such as evaporation, emulsification, dissolution, etc. which modifies particle properties.

Model area - Vatlestraumen

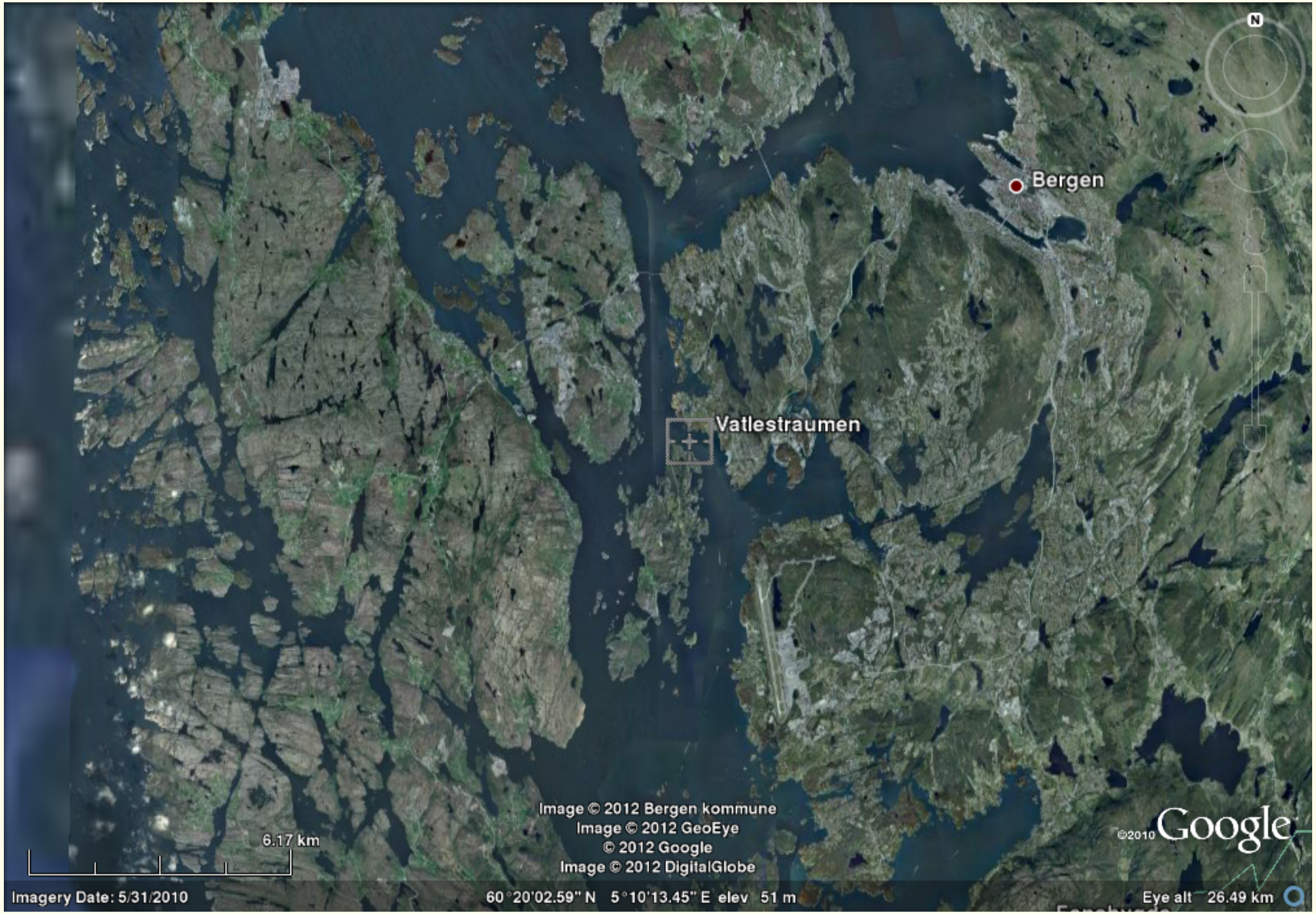

Model area - Vatlestraumen

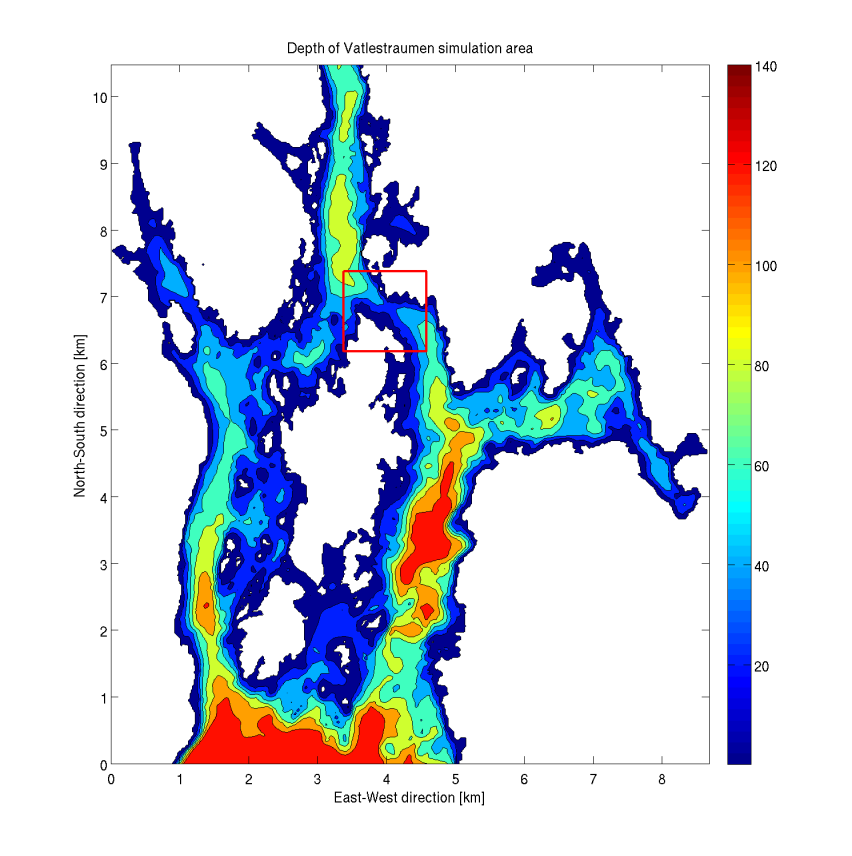

Topography of model area

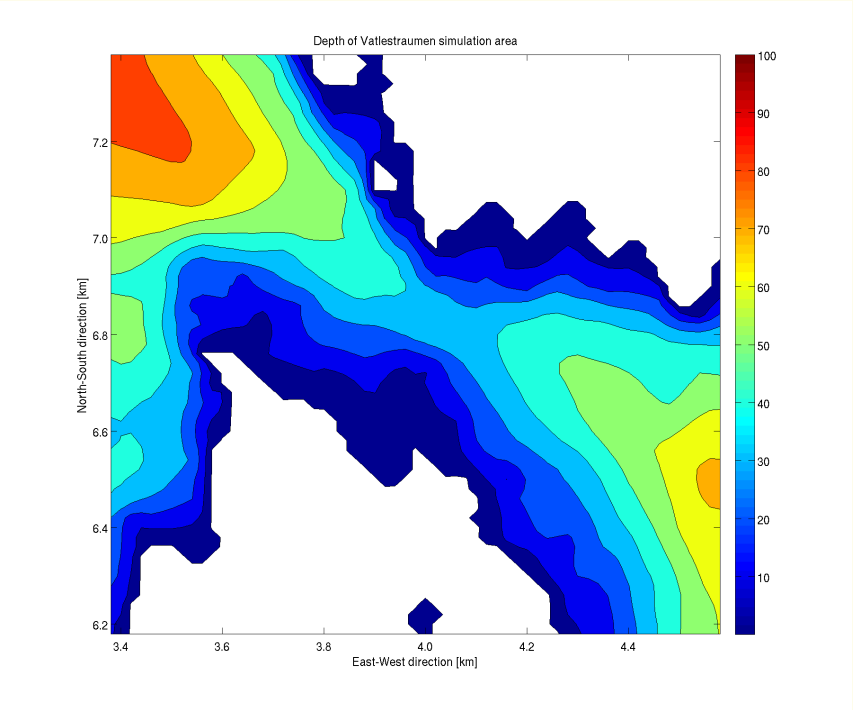

Detailed view of topography in Vatlestraumen

- Low resolution simulations: 80 m horizontal grid resolution, 10 sigma layers
- High resolution simulations: 20 m horizontal grid resolution, 31 sigma layers
- Bergen Ocean Model (BOM)
  - Numerical terrain-following 3D hydrodynamical model
  - Non-hydrostatic model equations; parallel code

Tidal current measurements

Data from Aanderaa instruments measurement site in Vatlestraumen

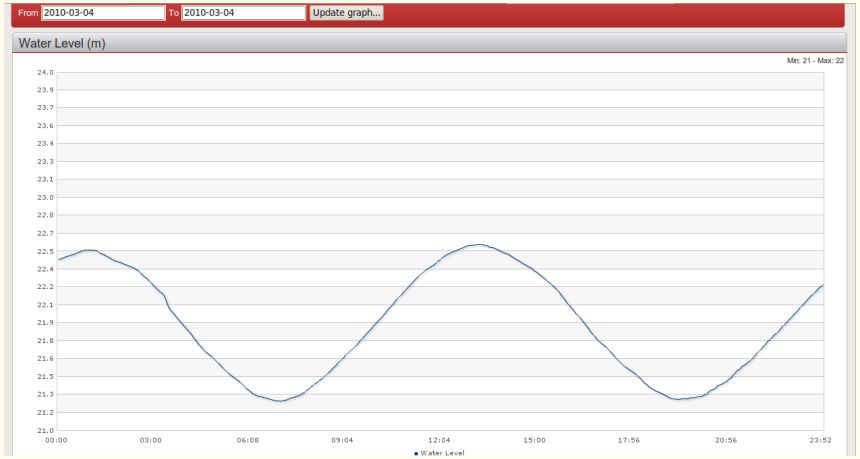

Water level 2010-03-04

Measurements show tidal water level change of about 1.2 m. Tidal water level change at the time of the accident is believed to be slightly less than 1 m.

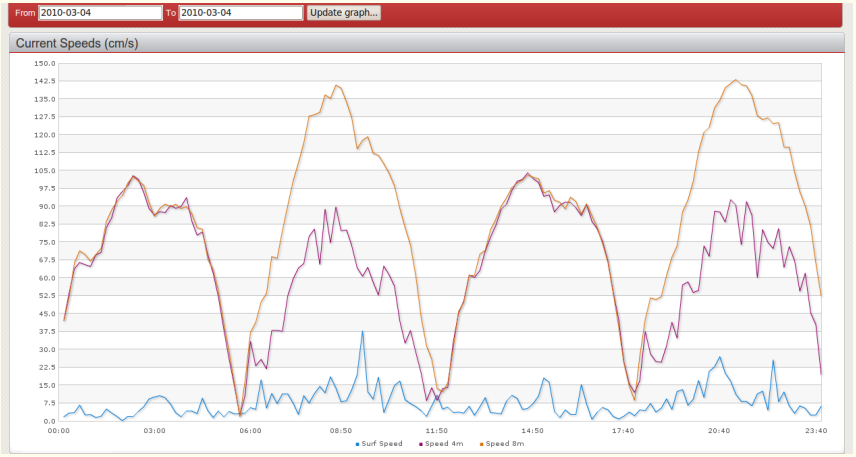

Current speed 2010-03-04

Current velocity measurements at surface (blue), 4 m depth (magenta) and 8 m depth (orange). Surface velocity data are probably wrong. Current speed measurements at 8 m depth regularly reach 0.8 m/s, with peaks exceeding 1 m/s.

Maximum northward current occurs approximately 1.5 hours after lowest tide.

”Oil spill” transport by particle tracking

- Simulation with 5000 particles, seeded at 3 m depth
- Constant horizontal eddy diffusion coefficients

$$A_H = 0.1 m^2/s \qquad K_H = 0 m^2/s$$

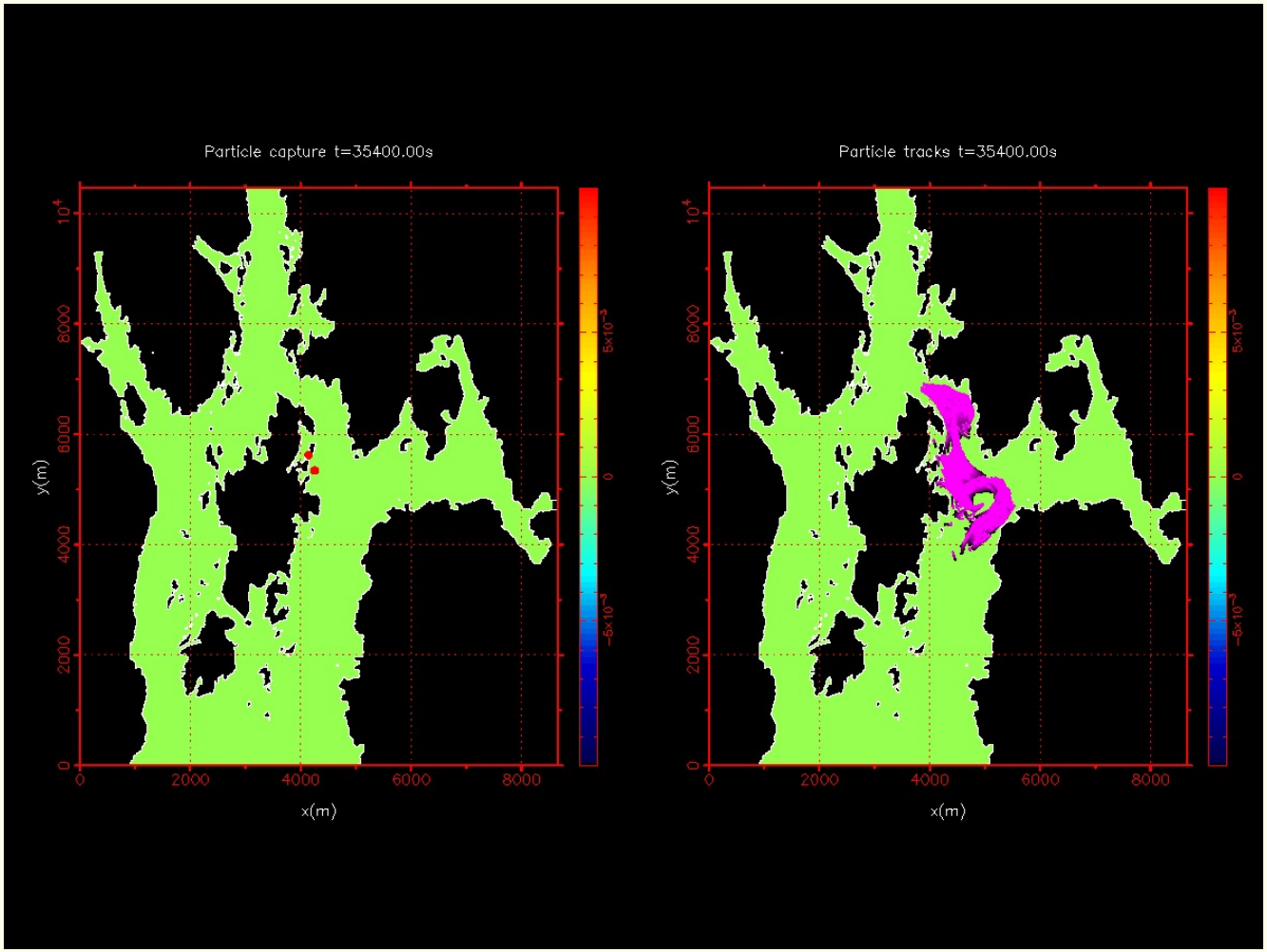

Extent of oil spill, January 20, 9:45 am

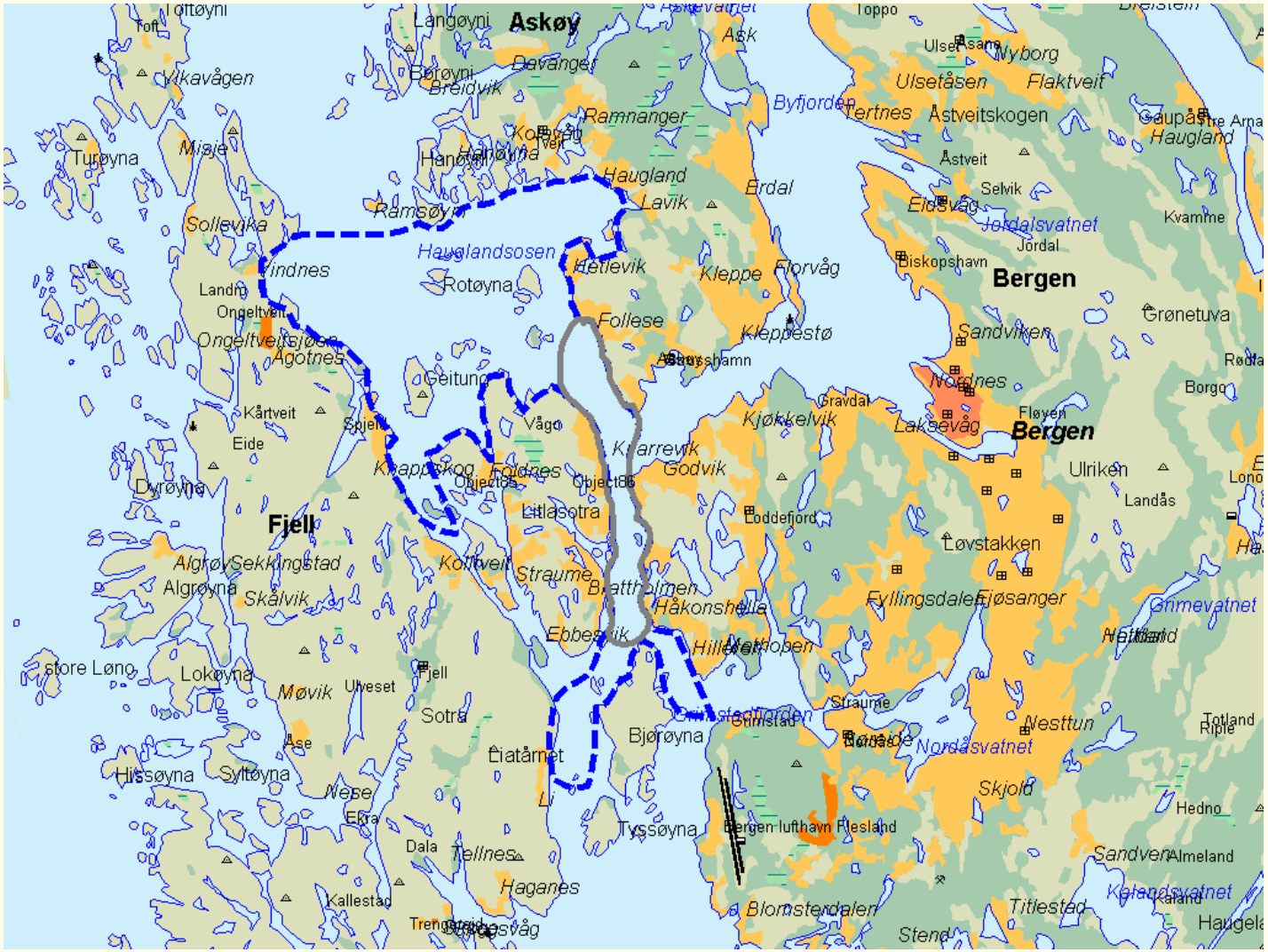

Source: ”ROCKNES”-ULYKKEN, The Norwegian Coastal Administration, 23. november 2004

Lagrangian coherent structures

Lagrangian Coherent structures (LCSs) are structures which separate dynamically distinct regions in time-varying systems.

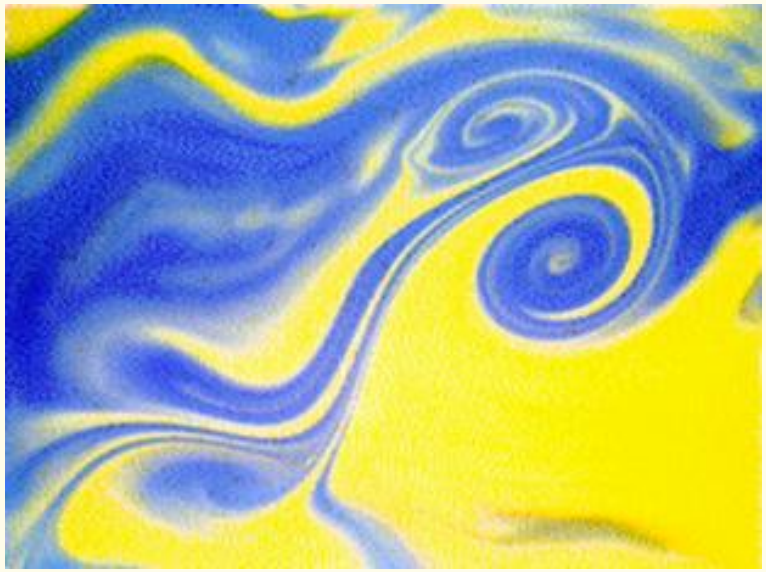

http://www.physics.mun.ca/ yakov/gallery.html

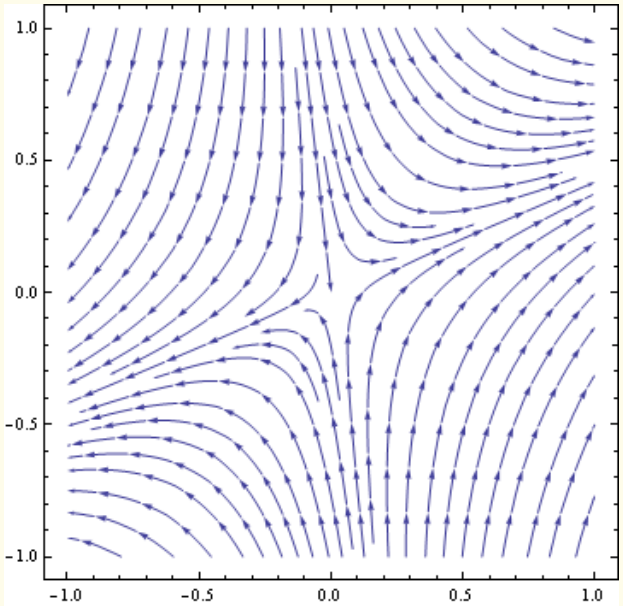

There is no commonly accepted definition for what constitutes a “coherent structure”, but extraction of CS from flow fields remains a fundamental goal for flow analysis.

LCSs are associated with identification of *hyperbolic points* (intersections of regions of divergence and convergence)

Lagrangian coherent structures

LCSs characterize the flow "skeleton"

Unstable and stable manifolds intersect at critical points. These manifolds can be interpreted as transport barriers.

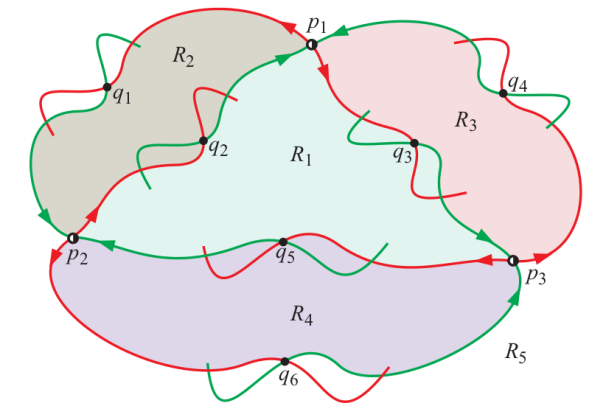

Transport barrier structures can be detected by use of Lyapunov exponents.

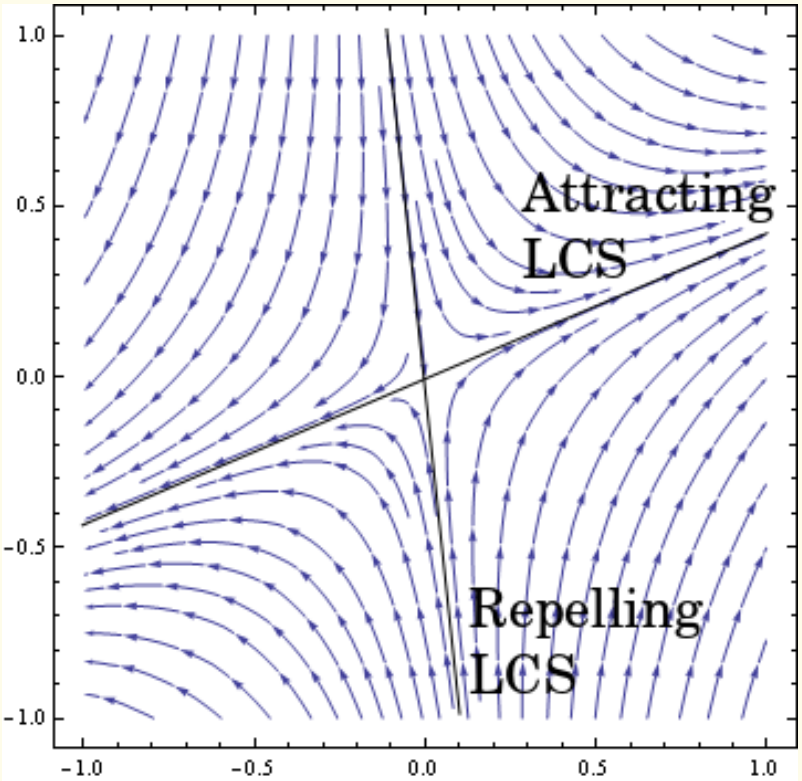

A critical point formed by attracting and repelling LCS

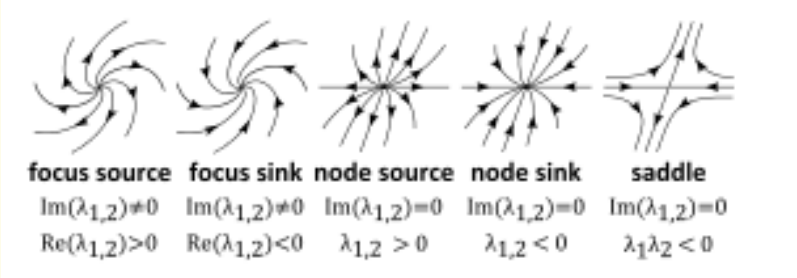

Types of first-order critical points in 2D

Lyapunov exponents

- Named after the Russian mathematician and physicist Aleksandr Mikhailovich Lyapunov (1857–1918).
- The Lyapunov exponent characterizes the rate of separation of initially close trajectories. Trajectories with initial separation distance δZ_0 diverge at a rate given by

$$|\delta Z(t)| \approx |\delta Z_0| \exp(\lambda t)$$

  where λ is the *Lyapunov exponent*.
- The rate of divergence depend on orientation of the initial separation vector. The maximum Lyapunov exponent can be defined as

$$\lambda_{max} = \lim_{t\to\infty} \lim_{\delta Z_0 \to 0} \frac{1}{t} \ln \frac{|\delta Z(t)|}{|\delta Z_0|}$$

Finite Lyapunov Exponents

In practical applications we wish to construct flow maps based on *local* Lyapunov exponents. There are several methods available:

- Direct Lyapunov Exponent (DLE) or (localized) Finite-Time Lyapunov Exponents (FTLE_L): Follow a single trajectory for a long time, and calculate the LE through eigenvalues of the Jacobian matrix $J(X_0)$.
- (Flowmap) Finite-Time Lyapunov exponent (FTLE_F): Calculate LE based on the dispersion of a cluster of particles.

For either method the calculation depends on a finite time of integration τ. This parameter should be selected based on the expected life time for coherent structures.

- Finite-Size Lyapunov Exponent (FSLE): Similar to FTLE_F, follows a cluster of particles until two trajectories have diverged by a specific distance (e.g. track patch until $\delta Z_1 = 2\delta Z_0$).

Lyapunov exponent: $\lambda = \tau \ln(\delta Z_1/\delta Z_0)$. For FTLE_F δZ_1 is determined by calculation, for FSLE τ is determined by calculation.

Finite-Time Lyapunov Exponents ($FTLE_F$)

- Track particle clusters over a finite time interval τ
- Calculate Lyapunov exponent based on the largest trajectory divergence in the cluster.

LCSs can be detected tracking clusters of particles throughout the computational domain. The time evolution of the LCS can be detected by computing FTLE fields for a sequence of overlapping time windows.

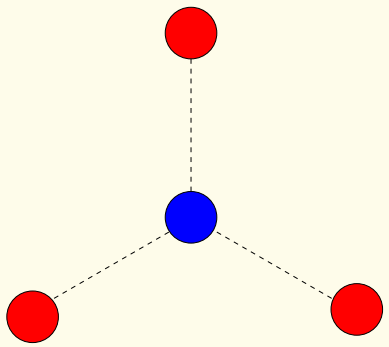

Particle cluster

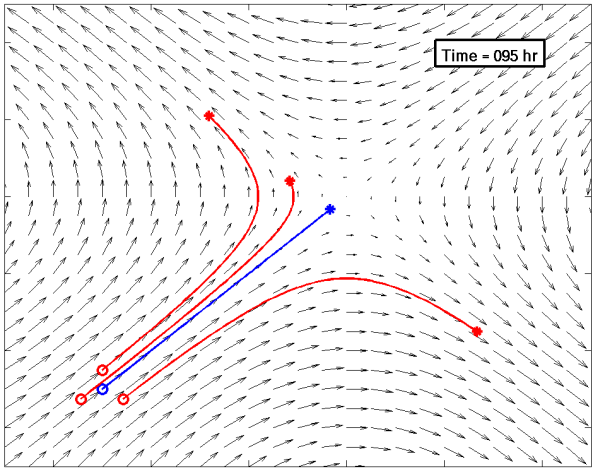

Evolution of particle cluster

Finite Time Lyapunov Exponents (FTLE_L)

- Calculations based on the (right) Cauchy-Green deformation tensor

$$\mathbf{C}_{t_0}^{t_0+\tau}(\mathbf{x_0}) = \left[\frac{\partial \mathbf{x}(\mathbf{x_0}, t_0, t_0+\tau)}{\partial \mathbf{x_0}}\right]^T \left[\frac{\partial \mathbf{x}(\mathbf{x_0}, t_0, t_0+\tau)}{\partial \mathbf{x_0}}\right]$$

- maximum FTLE

$$\mathrm{FTLE}_L^{t_0+\tau}(\mathbf{x_0}) = \frac{1}{2(t_0+\tau)} \ln \lambda_{\max}\left(\mathbf{C}_{t_0}^{t_0+\tau}\right)$$

where $\lambda_{\max}\left(\mathbf{C}_{t_0}^{t_0+\tau}\right)$ is the maximum eigenvalue of $\mathbf{C}_{t_0}^{t_0+\tau}$

FTLE_L over 6 hours

25 hours

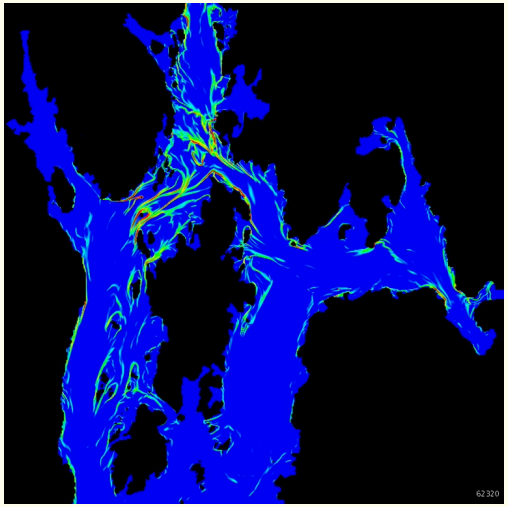

26 hours

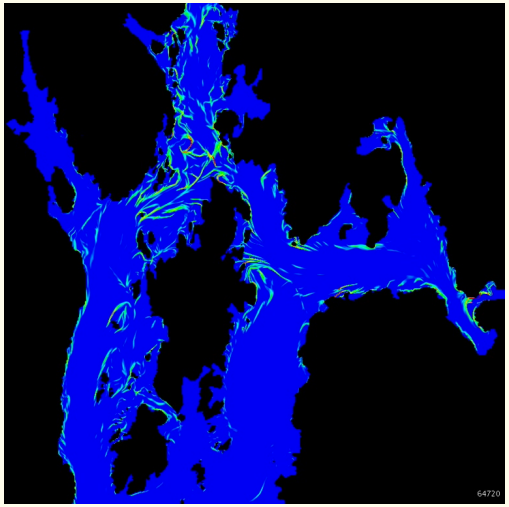

27 hours

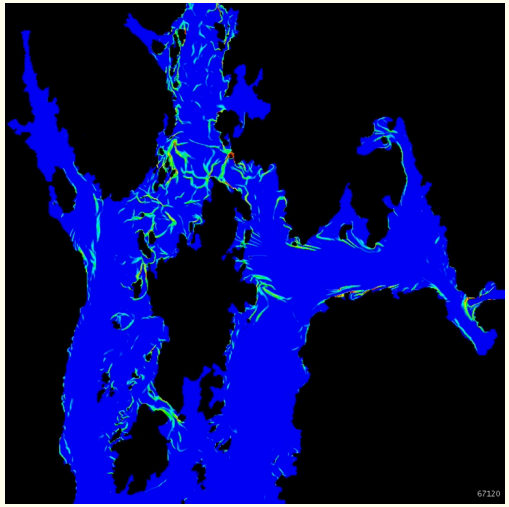

28 hours

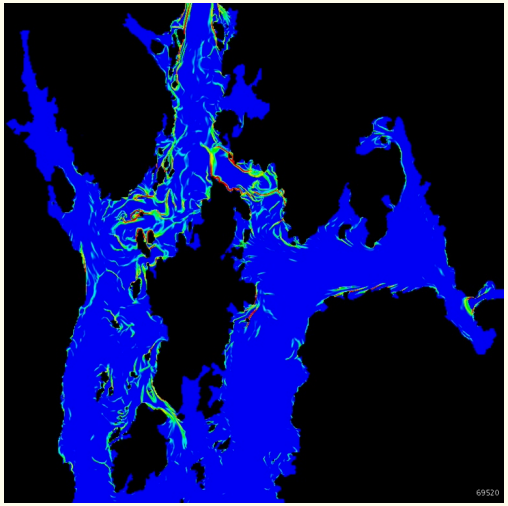

29 hours

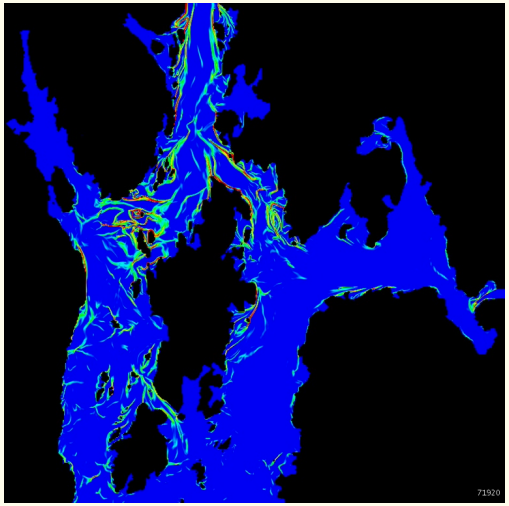

30 hours

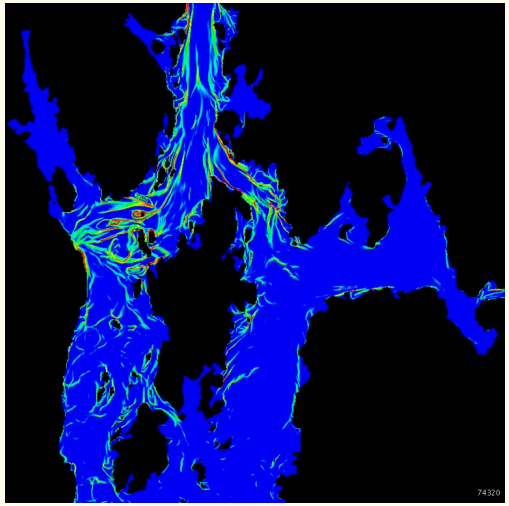

Results for FTLE obtained by off-line trajectory model, using time window $\tau = 30$ min.

Okubo-Weiss parameter

Okubo-Weiss parameter

$$W = s_n^2 + s_s^2 - \omega^2$$

where

$$s_n = \frac{\partial u}{\partial x} - \frac{\partial v}{\partial y} \quad \text{normal strain}$$

$$s_s = \frac{\partial v}{\partial x} + \frac{\partial u}{\partial y} \quad \text{shear strain}$$

$$\omega = \frac{\partial v}{\partial x} - \frac{\partial u}{\partial y} \quad \text{relative vorticity}$$

- Analysis of output velocity fields from BOM.
- Provides an instantaneous measure for the relative contribution of deformation and vorticity.

OW-parameter over 6 hours

Results for 80 m horizontal grid resolution.

25 hours

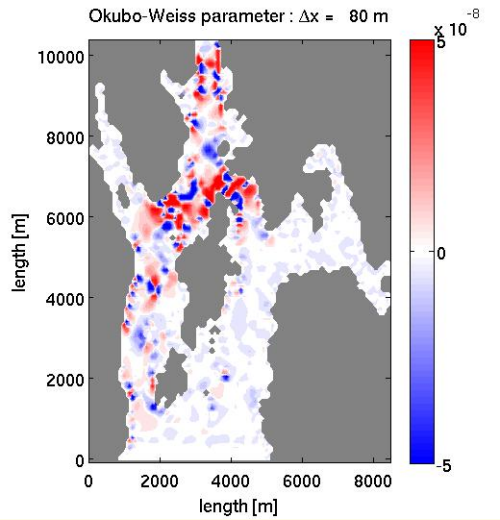

26 hours

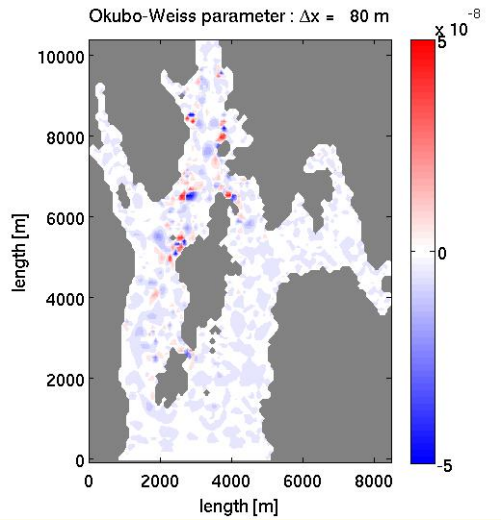

27 hours

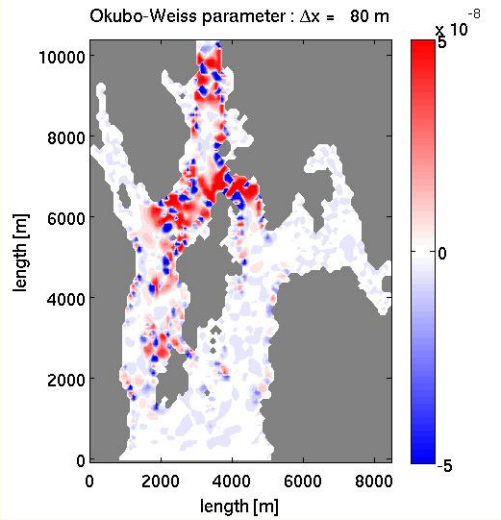

28 hours

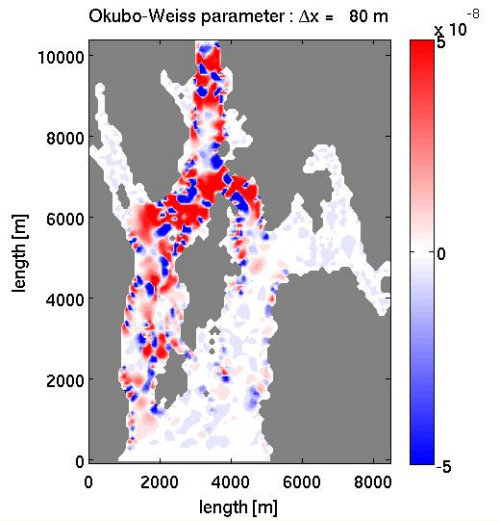

29 hours

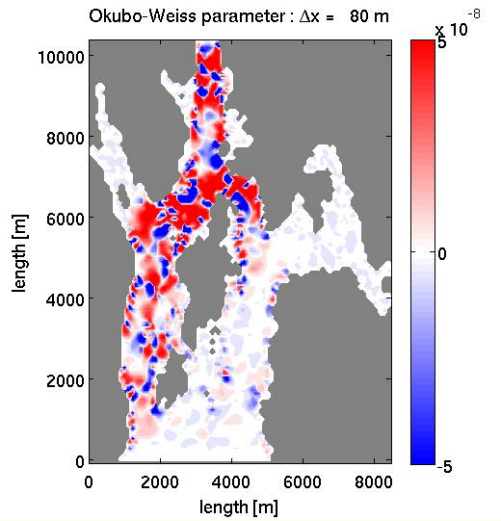

30 hours

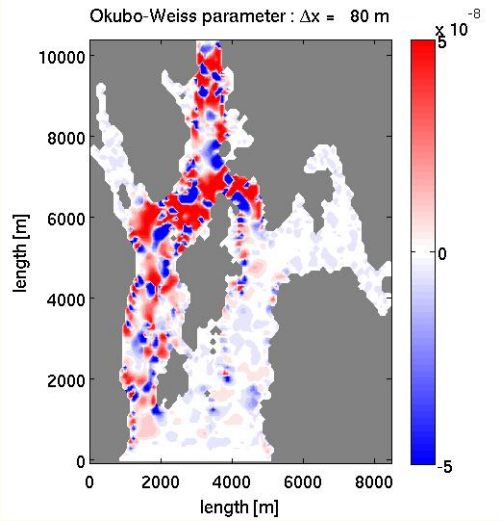

Comparing OW-parameter and FTLE

- The Okubo-Weiss parameter is a measure of the instantaneous separation rate.
- The FTLE gives the average, or integrated, separation between trajectories.
- FTLE is often more revealing than the OW-parameter because in time-dependent flows, the instantaneous streamlines can quickly diverge from particle trajectories. Since FTLE accounts for integrated flow effects it is more indicative of actual transport behavior.

References

Coherent structures:

- A. K. M. F. Hussain. Coherent structures - reality and myth. Physics of Fluids, 26:2816–2850, October 1983.
- A. K. M. F. Hussain. Coherent structures and turbulence. Journal of Fluid Mechanics, 173:303–356, 1986.

Finite-Time Lyapunov exponents:

- G. Haller. Finding finite-time invariant manifolds in two-dimensional velocity fields. Chaos, 10:99–108, March 2000.
- G. Haller. Distinguished material surfaces and coherent structures in three dimensional fluid flows. Physica D, 149(4):248–277, 2001.
- G. Haller. Lagrangian coherent structures from approximate velocity data. Physics of Fluids, 14:1851–1861, 2002.